P H Y S I C A L   R E V I E W   L E T T E R S

Origin of the Failure of Classical Nucleation Theory: Incorrect Description of the Smallest Clusters

Joonas Merikanto,[*] Evgeni Zapadinsky, Antti Lauri, and Hanna Vehkamäki

University of Helsinki, Department of Physical Sciences, P.O. Box 64, FIN-00014 University of Helsinki, Finland

We carry out molecular Monte Carlo simulations of clusters in an imperfect vapor. We show that down to very small cluster sizes, classical nucleation theory built on the liquid drop model can be used very accurately to describe the work required to add a monomer to the cluster. However, the error made in modeling the smallest of clusters as liquid drops results in an erroneous absolute value for the cluster work of formation throughout the size range. We calculate factors needed to correct the cluster formation work given by the liquid drop model. The corrected work of formation results in nucleation rates in good agreement with recent nucleation experiments on argon and water.

A better understanding of the limiting step in a phase transition, the nucleation process, is vital for a wide range of fields from nanotechnology and medical engineering to atmospheric sciences. Any application where nanoparticles are generated relies on understanding the nucleation process. The main uncertainty in global climate modeling is how radiative forcing is affected by aerosol particles, 30% of which are estimated to be produced by atmospheric nucleation [1]. The classical nucleation theory (CNT), based on the liquid drop (LD) model, is the main tool for calculations of nucleation rates in practically relevant systems. However, the magnitude and temperature dependency of the classical nucleation rate is often in contradiction with experiments. The discussion about the failure of CNT has focused on two possible explanations: CNT intrinsically miscalculates the degrees of freedom of nucleating clusters, and the use of LD model assigning macroscopic thermodynamic properties to molecular-size systems is inaccurate [2–4]. The detailed reasons for the failure of CNT are not, however, known.

In approaches based on molecular interactions the molecular clusters are properly treated as microscopic objects and the degrees of freedom can be correctly counted [5]. Classical molecular models use interaction potentials which cannot fully reproduce all the measured properties of the real substances. Most notably the value of the surface tension is often incorrect. Thus, a direct comparison between molecular simulations and experimental nucleation studies is not straightforward. Accurate quantum chemical calculations would avoid these problems, but have been considered computationally too expensive for studying the nucleation process. However, simulations with classical molecular models suggest that down to small critical cluster sizes the difference between the simulated and CNT nucleation barriers stays constant [6–9], and that very small molecular clusters exhibit macroscopic surface energy properties [10,11]. These results motivate us to study the minimum cluster size that can be treated without microscopic information.

There are several essentially equivalent [12,13] Monte Carlo methods which can calculate the work of formation of molecular clusters. The method we use is described in detail in our earlier papers [12,13]. The number density of the critical clusters is calculated using the equilibrium cluster distribution

$$N_n = N_1 \exp\left(-\frac{\Delta W_n}{k_B T}\right), \tag{1}$$

where n is the cluster size, k_B is the Boltzmann constant, and T is temperature. Equation (1) holds both for CNT and molecular approaches, and the difference lies in the method of calculating the value ΔW_n, often referred to as the work of cluster formation. In CNT, ΔW_n is given by

$$\Delta W_{n,\text{LD}} = A_n \gamma_\infty + n(\mu_l - \mu_v), \tag{2}$$

where A_n is the surface area given by the LD model, which also assigns the macroscopic surface tension γ_∞ to this surface, and μ_l and μ_v are the bulk liquid and vapor chemical potentials, respectively. The above expression also assigns an unphysical nonzero work of formation for a monomer. Defining the vapor saturation ratio as $S = \exp[(\mu_v - \mu_l)/k_B T]$, the change in cluster work of formation with respect to cluster size n is given by CNT as

$$\delta \Delta W_{n,\text{LD}} = \Delta W_{n,\text{LD}} - \Delta W_{n-1,\text{LD}}$$
$$= [n^{2/3} - (n-1)^{2/3}]A_1 \gamma_\infty - k_B T \ln S. \tag{3}$$

The above expression is valid at the bulk limit. Therefore, for an equilibrium vapor $\delta \Delta W_{n,\text{LD}}$ goes to zero once the cluster size becomes infinitely large ($n \to \infty$) and its surface becomes planar. The classical values of $\Delta \delta W_{n,\text{LD}}$ for $n \geq 2$ are used also in the self-consistent CNT [14] (SC-CNT), where $\Delta W_{n,\text{SC-CNT}} = \Delta W_{n,\text{LD}} - A_1 \gamma_\infty$, and McGraw-Laaksonen (ML) scaling theory [6] for nucleation barrier $\Delta W^*_{n,\text{ML}} = \Delta W^*_{n,\text{LD}} - D(T)$, where $D(T)$ is a function of temperature only. These models differ from CNT only by the value assigned to $\delta \Delta W_1 = \Delta W_1$.

In our simulation method $\delta\Delta W_n$ is calculated from

$$\delta\Delta W_{n,\text{sim}} = -k_B T \ln\frac{\bar{G}_{n-1}(T, \mu_v)}{\bar{D}_n(T, \mu_v)}, \quad (4)$$

where $\bar{G}_n$ and $\bar{D}_n$ are the grand canonical growth and decay probabilities averaged over all sampled configurations. The cluster configurations are generated according to the canonical Metropolis Monte Carlo scheme, and acceptable configurations are identified according to the Stillinger cluster definition. The physical interpretation of $\delta\Delta W_{n,\text{sim}}$ is the following: it is the work of bringing a monomer from infinity (vapor) to an $(n-1)$ cluster. The total work $\Delta W_{n,\text{sim}}$ represents the sum over all steps of creating an n cluster from monomers, $\Delta W_{n,\text{sim}} = \sum_{n'=2}^{n} \delta\Delta W_{n',\text{sim}}$. Note that in Monte Carlo methods the work of formation of a monomer cluster, $\Delta W_{1,\text{sim}}$, is taken as zero.

Earlier [12], we have shown that simulations carried out at chemical potential μ_{v1} can be scaled to another chemical potential μ_{v2}. The scaling law is given by

$$\frac{\bar{G}_{n-1}(T, \mu_{v2})}{\bar{D}_n(T, \mu_{v2})} = \exp\left(\frac{\mu_{v2} - \mu_{v1}}{k_B T}\right)\frac{\bar{G}_{n-1}(T, \mu_{v1})}{\bar{D}_n(T, \mu_{v1})}. \quad (5)$$

If we set μ_{v1} to μ_l, the exponential term in the above equation represents the saturation ratio S of vapor with chemical potential μ_{v2}. Thus, the work of formation can be written as

$$\Delta W_{n,\text{sim}} = -k_B T \sum_{n'=2}^{n} \ln\left[\frac{\bar{G}_{n'-1}(T, S=1)}{\bar{D}_{n'}(T, S=1)}\right]$$
$$- k_B T(n-1)\ln S. \quad (6)$$

Substituting Eq. (6) into Eq. (1) then gives

$$N_{n,\text{sim}} = \frac{N_1}{S}\exp\left[\sum_{n'=2}^{n}\ln\left(\frac{\bar{G}_{n'-1}(T, S=1)}{\bar{D}_{n'}(T, S=1)}\right) + n'\ln S\right]. \quad (7)$$

In the above equation the $1/S$ factor [4], appears naturally, and since $\Delta W_{1,\text{sim}} = 0$, Eq. (7) provides an internally consistent expression for the number of monomers. The exponent term in Eq. (7) can be viewed as the conventional expression for the work of cluster formation, $\Delta W_{n,\text{sim}}^{\text{conv}}$, which is of the same form as $\Delta W_{n,\text{LD}}$. The nucleation rate is calculated from $J = (K/S)\exp(\Delta W_{n^*}^{\text{conv}}/kT)$, where K is the classical prefactor and refers to the critical size.

We study the change in cluster work of formation with respect to cluster size $\delta\Delta W_{n,\text{sim}}$ both in Lennard-Jones (LJ) and water vapors. LJ clusters between sizes 1–200 are simulated at reduced temperatures $[T(K)/\epsilon$, where ϵ is the LJ energy parameter] 0.40, 0.44, 0.47, 0.50, 0.70, and 0.80. The water clusters are simulated with a polarizable water model by Guillot and Guissani (GG) [15] and non-polarizable four-point transferable intermolecular potential (TIP4P) and extended single point charge (SPC/E) models. GG and TIP4P simulations were carried out for clusters

containing 1–125 molecules at temperatures 220 K, 260 K, and 298.15 K. Simulations with SPC/E model were carried out at 298.15 K.

For larger cluster sizes the resulting $\delta\Delta W_{n,\text{sim}}^{\text{conv}}$ curves produce straight lines on $n^{2/3} - (n-1)^{2/3}$ scale, which correspond to the change of cluster surface area in the liquid drop model. For a unique value of μ_v, the lines cross the y axis at the origin. These curves, shown in Figs. 1(a) for LJ potential and 1(b) for GG water model, now correspond to the equilibrium vapor ($\mu_{v2} = \mu_v^e = \mu_l$). The behavior of $\delta\Delta W_n$ for TIP4P and SPC/E models is essentially identical to the results shown for GG model. The resulting saturated ideal gas densities $N_v^e = \exp(\mu_v^e/kT)$ match those obtained from Gibbs ensemble simulations [9,16]. According to LD model, the slope of $\delta\Delta W_n$ in Fig. 1 is determined by the surface energy $A_1\gamma_\infty$. The surface area of a monomer A_1 can be evaluated since the bulk liquid density is known from Gibbs ensemble simulations. Thus, γ_∞ can be extracted from the linear part of $\delta\Delta W_n$. Also the macroscopic surface tensions obtained from our simulations correspond to values from simulations of the bulk vapor-liquid interface. For example, for a LJ liquid at a reduced temperature of 0.7 and TIP4P model at 298.15 K we get $\gamma_{\infty,\text{LJ}} = 1.148$ (reduced units) and $\gamma_{\infty,\text{TIP4P}} = 57.9$ mN/m, while the reported values are $\gamma_{\infty,\text{LJ}} = 1.147$ (reduced units) [9] and $\gamma_{\infty,\text{TIP4P}} = 56 \pm 3$ mN/m [17], respectively. Note that our
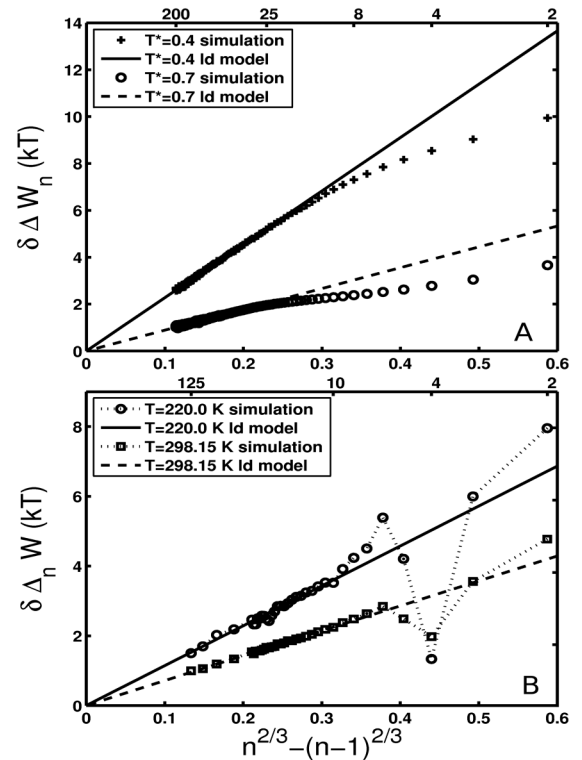

FIG. 1. The simulated and classical $\delta\Delta W_n^{\text{conv}}(S=1)$ for (a) Lennard-Jones clusters at reduced temperatures 0.4 and 0.7, and (b) water clusters using GG model at temperatures 220 and 260 K. The corresponding n values are shown on the top x axis.

analysis allows us to conveniently explore temperature regions where the bulk phases are those of solid and vapor, while clusters are still liquidlike; this is the case in nucleation experiments both with water and argon, to which we compare our results, and indeed such a situation is often encountered in vapor-liquid nucleation experiments.

The threshold number of molecules n^{thr} in the cluster, after which the linear behavior is observed, is in Lennard-Jones simulations between 25 ($T^* = 0.4$) and 50 ($T^* = 0.8$). The water simulations with all three water models produce a threshold size between 8 and 10 molecules for all simulated temperatures. For clusters below the threshold sizes significant deviations from LD model predictions are seen. The significant quantity describing the deviation of cluster properties from bulk liquid is the work of bringing a monomer from vapor to an ($n - 1$) cluster, $\delta\Delta W_n$. The error in the predictions of LD model arises from two effects which do not cancel each other: the real $\delta\Delta W_n$ is not linear for small clusters, and the erroneous nonzero value $A_1\gamma_\infty$ is assigned to the monomer work of formation. The breakdown of the model at small cluster sizes leads directly to a miscalculation of the density of larger clusters in the vapor since ΔW_n is calculated by summing $\delta\Delta W_n$ up from $n = 1$. The deviation from the LD model may be expressed as

$$\sum_{n'=1}^{n} [\delta\Delta W_{n',LD} - \delta\Delta W_{n',\text{sim}}^{\text{conv}}] = A_1\gamma_\infty + \sum_{n'=2}^{n} b_{n'}, \quad (8)$$

where the components b_n describe the deviation between $\delta\Delta W_{n,LD}$ and $\delta\Delta W_{n',\text{sim}}^{\text{conv}}$ shown in Fig. 1 for LJ potential and water. For a spherically symmetric LJ potential b_n is a smooth function of cluster size, but for water it is not; the dip at $n = 4$ seen in Fig. 1(b) results from a relatively stable cyclic ring structure where the water molecules are connected with hydrogen bonds. The structural issues govern b_n for complex molecules, and are more pronounced at low temperatures. However, above the threshold size the clusters are liquidlike, $b_{n\geq n^{trh}} = 0$ and $\sum_{n=2}^{n\geq n^{trh}} b_n = B(T)$, where $B(T)$ is size independent. The work of formation of clusters above the threshold size is given by

$$\Delta W_{n\geq n^{trh},\text{sim}}^{\text{conv}} = \Delta W_{n,LD} - A_1\gamma_\infty - B(T). \quad (9)$$

Therefore, our analysis reveals how SC-CNT, valid for a monomer cluster, evolves to the ML scaling theory where $D(T) = A_1\gamma_\infty - B(T)$, valid for clusters larger than n^{trh}.

The size dependence of surface tension acting on an equimolar surface can be calculated from

$$\gamma_e(n) = \frac{\Delta W_{n,\text{sim}}^{\text{conv}}(S=1)}{A_n} = \gamma_\infty - \frac{A_1\gamma_\infty + \sum_{n'=2}^{n} b_{n'}}{A_n}$$

$$(10)$$

which is in close connection to the ML expression [7] $\gamma_e(n) = \gamma_\infty - D(T)/A_n$. Figure 2 shows the calculated surface tension for small LJ clusters as a function of cluster size. Also the Tolman expression [18] $\gamma_e(n) =$
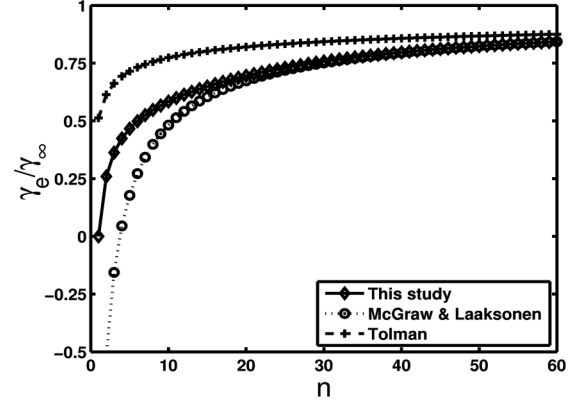

FIG. 2. Surface tension on equimolar surface as a function of cluster size for LJ clusters at $T^* = 0.7$ as calculated from Eq. (10), ML expression, and Tolman expression with a recent approximation $\delta_\infty = 0.16\sigma$ [22].

$\gamma_\infty(1 - 2\delta_\infty/R_n)$, truncated to first order in $1/R_n$, is shown for comparison. However, results from Tolman expression vary greatly with the applied value for δ_∞. Our calculated surface tension agrees with the ML expression above the threshold size, but deviates from it at smaller sizes, tending to zero for a monomer cluster.

By calculating $B(T)$ for LJ and for water clusters simulated with three potential models, we learned that $B(T)$ varies by less than $1k_BT$ for different temperatures. Importantly, $B(T) \approx 0$ for all the water models, while the calculated surface tensions between the models differ significantly. For LJ clusters $B(T) \approx 13.6k_BT$.

We compare our simulation results to experiments by Fladerer and Strey [19] of argon onset pressures producing a nucleation rate of $J = 10^7$ s^{-1} cm^{-3}, and to experiments by Wölk and Strey [20] of water nucleation rates as a function of temperature and saturation ratio. We find that both for argon and water $n^* > n^{trh}$ at all experimental conditions. Since $B(T)$ is not sensitive to variation of surface tensions between the three water models, we may use Eq. (9) with $B = 0$ and the real water surface tension reported by Holten et al. [21]. For comparison with the argon experiments we use Eq. (9) with an experimental value of surface tension [19] with $B(T) = 13.6k_BT$ calculated from LJ simulations considering it as a first order correction: The LJ potential gives a slightly different value to the surface tension compared to experiments.

The experimental, CNT, SC-CNT, corrected CNT according to Reiss, Kegel, and Katz [4] (RKK) and our simulation-based results are shown in Fig. 3 for argon and water. Figure 3(a) shows that our simulation-based onset pressures differ by a constant $p \approx 2000$ Pa at all temperatures in the experimental range, while both CNT and RKK (calculated using approximated compressibility 2×10^{-11} Pa^{-1} for argon) clearly overestimate them. While representing the most coherent set of argon nucleation measurements, Fladerer and Strey point out that their data contain fairly large error margins towards higher onset
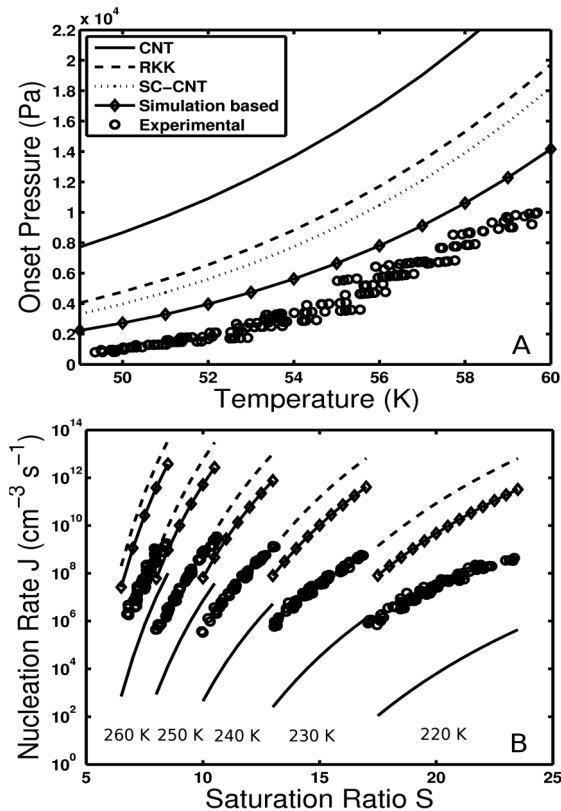
P H Y S I C A L R E V I E W L E T T E R S

FIG. 3. CNT, RKK, SC-CNT, simulation-based, and experimental results for (a) onset pressures producing argon nucleation rate 10^7 s^{-1} cm^{-3}, and (b) nucleation rates for water as a function of saturation ratio. For water SC-CNT and simulation-based results overlap.

pressures. The reported typical measuremental uncertainty can explain the difference between our results and measurements between 55 and 60 K.

Whereas the CNT, SC-CNT, and RKK predictions fail in case of argon, they are in a much better agreement with experimental measurements for water as shown in Fig. 3(b). Since we find $B(T) = 0$ for water, the simulation-based results are equal to the SC-CNT results in this case. Unlike CNT rates, the temperature dependencies of RKK and simulation-based rates are in good agreement with experiments, but some deviation in the saturation ratio dependency is seen in all cases. The simulation-based rates overestimate the experimental rates by 2−3 orders of magnitude depending on the saturation ratio. Overall, a comparison of our results to nucleation experiments explains why CNT fails to describe the nucleation of argon and gives a relatively successful description of the nucleation of water.

We have shown that the liquid drop model captures the work related to addition of a monomer to a cluster already above threshold cluster sizes between 8 to 50 molecules, depending on temperature and molecules in question. However, the microscopic effects related to the formation of the smallest clusters introduce a possibly large correc-

tion term to the total cluster work of formation given by CNT. The value of the correction term is constant for all clusters above the threshold size. Therefore, the critical cluster size does not pose a minimum size limit for the calculation of the correct critical cluster work of formation; for example, accurate quantum chemical calculations of 10 molecule water clusters are well achievable, and a physically sound correction to CNT can be obtained by studying only the smallest of clusters. This Letter shows how the most accurate molecular modeling methods can be exploited to essentially improve predictions of nanoparticle formation in practical applications.

*Electronic address: joonas.merikanto@helsinki.fi

[1] D. V. Spracklen, K. S. Carslaw, M. Kulmala, V.-M. Kerminen, G. W. Mann, and S.-L. Sihto, Atmos. Chem. Phys. **6**, 5631 (2006).
[2] J. Lothe and G. M. Pound, J. Chem. Phys. **36**, 2080 (1962).
[3] A. Dillmann and G. E. A. Meier, J. Chem. Phys. **94**, 3872 (1991).
[4] H. Reiss, W. K. Kegel, and J. L. Katz, Phys. Rev. Lett. **78**, 4506 (1997).
[5] J. K. Lee, J. A. Barker, and F. F. Abraham, J. Chem. Phys. **61**, 1221 (1974).
[6] R. McGraw and A. Laaksonen, Phys. Rev. Lett. **76**, 2754 (1996).
[7] R. McGraw and A. Laaksonen, J. Chem. Phys. **106**, 5284 (1996).
[8] P. R. ten Wolde and D. Frenkel, J. Chem. Phys. **109**, 9901 (1998).
[9] B. Chen, J. I. Siepmann, K. J. Oh, and M. L. Klein, J. Chem. Phys. **115**, 10903 (2001).
[10] B. N. Hale, Aust. J. Phys. **49**, 425 (1996).
[11] B. N. Hale and D. DiMattio, in *Proceedings of the 15th International Conference on Nucleation and Atmospheric Aerosols*, edited by B. Hale and M. Kulmala (Springer-Verlag, Berlin, 2000), p. 31.
[12] A. Lauri, J. Merikanto, E. Zapadinsky, and H. Vehkamäki, Atmos. Res. **82**, 489 (2006).
[13] J. Merikanto, E. Zapadinsky, and H. Vehkamäki, J. Chem. Phys. **121**, 914 (2004).
[14] S. L. Girshick and C. P. Chiu, J. Chem. Phys. **93**, 1273 (1990).
[15] B. Guillot and Y. Guissani, J. Chem. Phys. **114**, 6720 (2001).
[16] R. F. Cracknell, D. Nicholson, and N. C. Parsonage, Mol. Phys. **71**, 931 (1990).
[17] B. Chen, J. I. Siepmann, and M. L. Klein, J. Phys. Chem. A **109**, 1137 (2005).
[18] R. C, Tolman, J. Phys. Chem. **17**, 333 (1949).
[19] A. Fladerer and R. Strey, J. Chem. Phys. **124**, 164710 (2006).
[20] J. Wölk and R. Strey, J. Phys. Chem. B **105**, 11683 (2001).
[21] V. Holten, D. G. Labetski, and M. E. H. van Dongen, J. Chem. Phys. **123**, 104505 (2005).
[22] A. E. Giessen and E. M. Blokhuis, J. Chem. Phys. **116**, 302 (2002).